

Journal Pre-proof

Epidermal microorganisms contributed to the toxic mechanism of nZVI and TCEP in earthworms by robbing metal elements and nutrients

Jie Hou, Meirui Yang, Xinyue Wu, Qiqi Chen, Yuqi Lu, Jianying Zhang, Daohui Lin



PII: S2772-9850(23)00068-6

DOI: <https://doi.org/10.1016/j.eehl.2023.11.001>

Reference: EEHL 72

To appear in: *Eco-Environment & Health*

Received Date: 4 September 2023

Revised Date: 16 October 2023

Accepted Date: 14 November 2023

Please cite this article as: J. Hou, M. Yang, X. Wu, Q. Chen, Y. Lu, J. Zhang, D. Lin, Epidermal microorganisms contributed to the toxic mechanism of nZVI and TCEP in earthworms by robbing metal elements and nutrients, *Eco-Environment & Health*, <https://doi.org/10.1016/j.eehl.2023.11.001>.

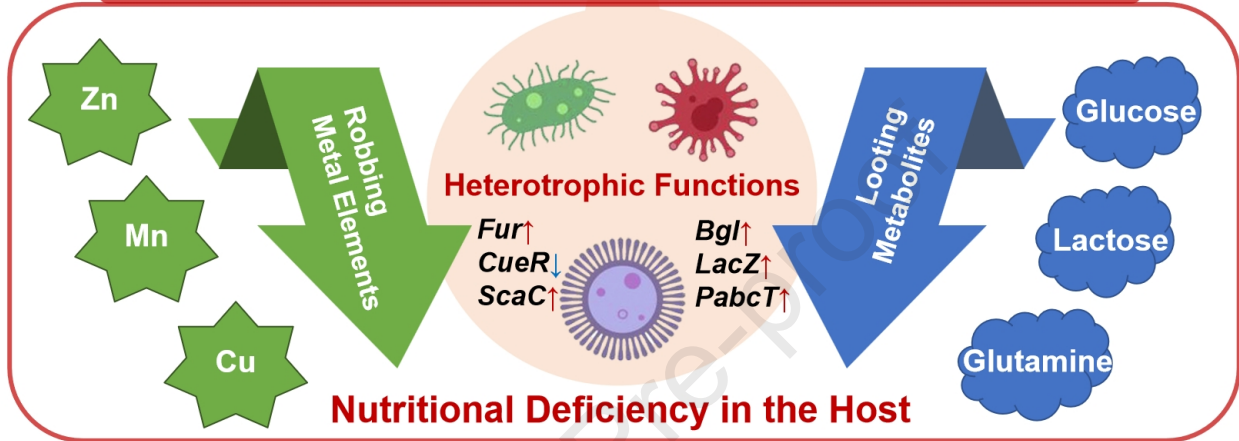
This is a PDF file of an article that has undergone enhancements after acceptance, such as the addition of a cover page and metadata, and formatting for readability, but it is not yet the definitive version of record. This version will undergo additional copyediting, typesetting and review before it is published in its final form, but we are providing this version to give early visibility of the article. Please note that, during the production process, errors may be discovered which could affect the content, and all legal disclaimers that apply to the journal pertain.

© 2023 The Author(s). Published by Elsevier B.V. on behalf of Nanjing Institute of Environmental Sciences, Ministry of Ecology and Environment (MEE) & Nanjing University.

Co-contamination in Soil



Epidermal Microorganisms Dominated Toxic Mechanisms



1 **Epidermal microorganisms contributed to the toxic mechanism of nZVI and TCEP in**
2 **earthworms by robbing metal elements and nutrients**

3 Jie Hou^{a,1}, Meirui Yang^{a,1}, Xinyue Wu^a, Qiqi Chen^a, Yuqi Lu^a, Jianying Zhang^{a,c}, Daohui Lin^{a,b*}

4 ^a Zhejiang Provincial Key Laboratory of Organic Pollution Process and Control, Department of
5 Environmental Science, Zhejiang University, Hangzhou 310058, China

6 ^b Zhejiang Ecological Civilization Academy, Anji 313300, China

7 ^c National Demonstration Center for Experimental Environment and Resources Education (Zhejiang
8 University), Hangzhou 310058, China

9
10 *Corresponding author: D.H. Lin (lindaohui@zju.edu.cn)

11 ¹ The two authors contributed equally to this work.

12 **Abstract**

13 Disrupting effects of pollutants on symbiotic microbiota have been regarded as an important
14 mechanism of host toxicity, with most current research focusing on the intestinal microbiota. In fact,
15 the epidermal microbiota, which participates in the nutrient exchange between hosts and
16 environments, could play a crucial role in host toxicity via community changes. To compare the
17 contributions of intestinal and epidermal symbiotic microorganisms to host toxicity, this study
18 designed single and combined scenarios of soil contamination [nano zero-valent iron and tris (2-
19 chloroethyl) phosphate], and revealed the coupling mechanisms between intestinal/epidermal
20 symbiotic bacterial communities and earthworm toxicological endpoints. Microbiome analysis
21 showed that 15% of intestinal microbes were highly correlated with host endpoints, compared to 45%
22 of epidermal microbes showing a similar correlation. Functional comparisons revealed that key
23 species on the epidermis were mainly heterotrophic microbes with genetic abilities to utilize metal
24 elements and carbohydrate nutrients. Further verifications demonstrated that when facing the co-
25 contamination of nZVI and TCEP, certain symbiotic microorganisms became dominant and
26 consumed zinc, copper, and manganese along with saccharides and amino acids, which may be
27 responsible for the nutritional deficiencies in the host earthworms. The findings can enrich the
28 understanding of the coupling relationship between symbiotic microorganisms and host toxicity,
29 highlighting the importance of epidermal microorganisms in host resistance to environmental

30 pollution.

31 **Keywords:** Microbial community; Host; Soil pollution; Joint toxicity; Heterotrophic function

32 1. Introduction

33 Organisms in nature do not exist independently but in the form of symbionts with
34 microorganisms [1,2]. As the second genome of the host, symbiotic microorganisms, including both
35 probiotics and pathogens, can regulate host health and thus contribute to the vulnerability of the host
36 under environmental stresses [3]. In the soil environment, earthworms and drilosphere
37 microorganisms coexist as classic and widespread symbionts, and their interactions deeply influence
38 earthworm tolerance to soil contamination [4]. Generally, symbiotic microorganisms are harbored
39 both in the gut and on the epidermis. Intestinal microorganisms play important roles in pathogen
40 inhibition and the maintenance of intestinal barrier functions, which have garnered much research
41 attention in recent years [5,6]. Different from the gut, the epidermis serves as a vital barrier against
42 external environmental threats, with its mucus layer providing an abundant nutritional source and
43 stable microhabitat for symbiotic bacterial colonization [7]. However, due to the complexity and
44 challenges associated with symbiotic microorganism separation and identification, existing
45 toxicology studies have mostly focused on the direct impact of pollutants on the host, leaving the role
46 of symbiotic microorganisms in host toxicity obscure.

47 Essentially, when contaminants induce host toxicity by disrupting symbiotic microorganisms,
48 the final effects depend on the community changes of symbiotic microorganisms along with their
49 functions. Certain microorganisms may strengthen or weaken the resistance of the host to external
50 pollutants by modulating nutrient cycling, absorption of essential elements, and pollutant metabolism
51 [8-11]. For example, intestinal microbes have been observed to affect host nutrient cycling through
52 the synthesis of vitamins, short-chain fatty acids, and various gut hormones [8]. Previous research
53 has shown significant increases in the abundance of beneficial microbiomes, such as *Blautia* and
54 *Bifidobacterium*, induced by allicin (diallylthiosulfinate), in maintaining glucose homeostasis and
55 ameliorating hepatic steatosis [11]. Concurrently, symbiotic microorganisms also regulate the
56 absorption and homeostasis of essential host elements, influencing the pollution tolerance of the host
57 via specific functional proteins. For instance, iron is essential to host immunity, and bacteria can
58 manage intracellular iron storage and release at the molecular level through various receptors, thereby
59 affecting host iron homeostasis and health [12]. On the other hand, recent findings showed that

60 carbon/nitrogen metabolites generated by earthworms, such as S-(2-hydroxyethyl) glutathione, 16-
61 hydroxypalmitic acid, and formamide, could be particularly utilized by microorganisms when
62 exposed to polychlorinated biphenyls (PCBs) at environmental concentrations in soil [13]. As
63 favorable carbon/nitrogen sources for microorganisms, these substances stimulated the colonization
64 of the PCB-degrading bacteria *Novosphingobium* and *Achromobacter* in the gut, thus bolstering the
65 resistance of earthworms to PCB pollution in soil. At present, toxicological studies on symbiotic
66 microorganisms are merely focused on gut flora, while the response mode of epidermal
67 microorganisms to pollutants, along with their contribution to host toxicity, remains largely unclear.
68 Systematic comparisons using big data tools are urgently needed, especially on the structure–function
69 relationship between the community composition of epidermal microorganisms and their biological
70 interactions with the host.

71 In the present study, we hypothesized that epidermal microorganisms, which play a crucial role
72 in mediating direct contact between the host and the environment, may contribute to host toxicity via
73 their community responses under environmental stresses. To distinguish the contributions of intestinal
74 and epidermal symbiotic microorganisms to host toxicity, we designed single and combined scenarios
75 of soil contamination using nano zero-valent iron (nZVI) and tris (2-chloroethyl) phosphate (TCEP)
76 as representatives of emerging nanoparticulates and organic contaminants [14,15], and investigated
77 the coupling mechanisms between the intestinal/epidermal symbiotic bacterial communities and the
78 earthworm physiochemical endpoints using 16S rRNA sequencing and metagenomic analysis
79 techniques. After identifying alterations in the community structure, we screened out key
80 microorganisms in the intestine and epidermis, and verified the relationship between their genetic
81 functions and the related host endpoints under co-contamination conditions.

82 **2. Materials and methods**

83 **2.1. Exposure experiment and host toxicity assays**

84 Earthworms (*Eisenia fetida*) were provided by a farm in Jiaying, China. Since TCEP pollution
85 has been threatening the agriculture near e-waste dismantling area, paddy soil was collected from a
86 farmland in Hangzhou, China, and was used as the culture matrix. TCEP and nZVI may coexist during
87 nZVI-based soil remediation, which was mimicked as a typical coexposure scenario [16, 17]. nZVI
88 with an approximate diameter of 80 nm was obtained from Hongwu Material Technology
89 (Guangzhou, China). The characterizations of soil and nZVI are shown in Supplementary material

90 Text S1. TCEP and its internal standard *d*12-TCEP were purchased from Toronto Research Chemicals
91 Company (Toronto, Canada). All organic solvents used in the study were of analytical grade. The
92 experiment followed the Organization for Economic Cooperation and Development (OECD)
93 Guideline 222. TCEP and nZVI were added to the soil to perform a 4 × 4 factorial experiment,
94 reaching desired concentrations of 50, 500, and 5,000 µg/kg and 50, 500, and 5,000 mg/kg,
95 respectively [15]. The concentration gradient was chosen according to the ambient concentration of
96 TCEP and the application dose of nZVI during typical soil remediations [16-18]. A 28-d exposure
97 was conducted in beakers, as detailed in Text S2. After exposure, ten earthworms were collected from
98 each group and kept on moist filter paper for 24 hours to clear their intestinal contents. Physiological
99 endpoints, including weight gain rate and food ingestion rate, were measured, and biochemical
100 indicators, including superoxide dismutase (SOD), catalase (CAT), malondialdehyde (MDA),
101 glutathione S-transferase (GST), reduced glutathione (GSH), and acetyl-cholinesterase (AChE), were
102 determined, as detailed in Text S3, Fig. S2 and our previous study [19].

103 **2.2. Microbiome analysis of symbiotic microorganisms**

104 Microbiota sampling from the secretion of the intestine and epidermis was performed under
105 sterile conditions. After exposure, earthworms were cleaned, freeze-dried, and preserved at -80 °C.
106 The sterilized earthworm was secured and incised to extract intestinal contents. The secretion of
107 intestine and epidermis of three earthworms were collected as one sample, and stored at -80 °C for
108 future analysis and sequencing. Each treatment group contained three replicates. Subsequent
109 microbial sequencing was conducted by Majorbio Bio-Pharm Technology Co. (Shanghai, China). In
110 detail, genomic DNA extracted from the samples was first analyzed via 1% agarose gel
111 electrophoresis, and only samples with an OD_{260/280} value over 1.8 were used. After that, a
112 quantitative real-time polymerase chain reaction (qPCR) was used for the amplification and
113 purification of the product. The product was then examined and quantified using a fluorescence
114 quantification system, and the Illumina library was constructed and sequenced. Resulting PE reads
115 were joined based on overlap while concurrently conducting sequence quality control and filtration.
116 A series of statistical and visual analyses, including the Venn diagram (Fig. S3), Principal Component
117 Analysis (PCA) (Fig. S4), hierarchical clustering tree (Fig. S5), and Community heatmap analysis
118 (Fig. S6), were carried out post-sample differentiation using the Majorbio Cloud Platform online tool
119 (<https://cloud.majorbio.com/page/tools/>).

120 **2.3. Determination of functional gene abundance**

121 According to the above microbiome analysis, epidermal microorganisms showing high
122 correlations with host toxicity were identified. Among these, *Brevundimonas*, *Microbacterium*,
123 *Mesorhizobium*, and *Ensifer* are well-known microorganisms, and their reported biological functions
124 are summarized in Table S1 based on the literature search. A heatmap was plotted by
125 <https://www.bioinformatics.com.cn>, an online platform for visualization of the relationship between
126 the epidermal microorganisms. To further quantify the microbial functions, genomic DNA was
127 analyzed using qPCR performed on an iQ5 Multicolor Real-Time PCR Detection System (Bio-Rad
128 Laboratories, Hercules, CA, USA). The degenerate primers of 10 genes [*Fur*, Ferric uptake regulator;
129 *Zur*, Zinc uptake regulator; *ZnuA*, Zinc ABC transporter substrate-binding protein; *CueR*, Cu(I)-
130 responsive transcriptional regulator; *ScaC*, scaffoldin anchoring protein C; *MntR*, Mn²⁺ transporter;
131 *Bgl*, beta-glucosidase; *LacZ*, beta-galactosidase; *NocR*, nucleoid occlusion protein regulatory protein;
132 *PabcT*, Peptide ABC transporter] related to metal-responsive proteins and saccharides/amino acids
133 uptake were designed using PRIMER 5.0 software based on the common sequences of detected
134 species (*Brevundimonas*, *Microbacterium*, *Mesorhizobium*, *Ensifer*, etc.) from the NCBI database
135 (Table S2). The relative abundance was calculated using the $2^{-\Delta\Delta Ct}$ method [20] and was visualized
136 using a heatmap according to the data in Table S3.

137 **2.4. Determination of TCEP contents**

138 The quantification of TCEP in earthworms was accomplished via extraction with acetonitrile.
139 The process was initiated by incorporating 0.2 g of earthworm tissue with 2 mL of acetonitrile and
140 20 ng of *d*12-TCEP employed as an internal standard. The subsequent supernatant was then subjected
141 to an ultrasonic extraction for 30 minutes, followed by a 10-minute centrifugation (3,000 rpm). This
142 process was iteratively performed thrice, after which the cumulated supernatant was desiccated to
143 near-dryness under a nitrogen flow of 1.0 mL/min. The resulting residue was then re-dissolved with
144 a 1:1 acetonitrile-water mix, followed by dilution to a predetermined range after filtration via a 0.22
145 μm organic PTFE filter. The TCEP analysis was conducted using the ACQUITY UPLC I-Class
146 system (Milford, MA, USA) on ACQUITY UPLC BEH C18 columns (2.1 mm \times 100 mm \times 1.7 μm)
147 coupled with an AB Sciex QTrap 5500 system (Foster City, CA, USA) using the multiple reaction
148 monitoring (MRM) acquisition mode under positive iron mode (ESI+). An elution gradient was then
149 implemented, using 50% formic acid in water (A) and 50% formic acid in acetonitrile (B), at a flow
150 rate of 0.2 mL/min, maintained for 8 minutes.

151 **2.5. Determination of elements**

152 Considering symbiotic microorganisms could regulate the absorption and homeostasis of
153 essential host elements and therefore contribute to host toxicity, non-metallic elements and metallic
154 elements, including Na, K, Ca, Mg, P, Zn, Mn, Fe, and Cu, were selected, and their alterations in
155 earthworms were measured after exposure to nZVI, TCEP, and their combination (nZVI-TCEP). In
156 each treatment group, earthworm bodies from three individuals were comprehensively digested
157 employing 6.0 mL concentrated HNO₃ and 2.0 mL H₂O₂ in a CEM Mars 4 microwave digestion
158 system (USA). The acid was reduced to a volume before being brought up to a 50 mL volume using
159 2% dilute HNO₃ for measurements. Quantification of Na, K, Ca, Mg, P, Zn, Mn, Fe, and Cu was
160 conducted using an inductively coupled plasma mass spectrometer (ICP-MS) (PerkinElmer NexION
161 300X, USA).

162 **2.6. Determination of saccharides and amino acids**

163 In each treatment group, three earthworms were homogenized manually in a vitreous tissue
164 homogenizer with phosphate-buffered saline (1:9). Homogenates were centrifuged at 4 °C for 15 min
165 at 3,000 rpm. D-glucose, lactose, and glutamine were measured using reagent kits from Jiangcheng
166 Bioengineering Institute (Nanjing, China) and Abnova Corporation (Wuhan, China), following the
167 manufacturer's instructions. In detail, D-glucose was measured by the glucose-oxidase method [21].
168 Lactose was broken down into galactose and glucose by β -galactosidase and then quantified by the
169 glucose oxidase method [21]. The measurement of glutamine was based on the signal at 565 nm when
170 glutamine was hydrolyzed to glutamate [22].

171 **2.7. Data analyses**

172 Data were analyzed using SPSS 26.0 and presented as mean \pm standard deviation (SD). Three
173 replicates were used for each treatment group in microbiome, gene abundance, and chemical/element
174 assays. Normality and variance homogeneity were verified before conducting a one-way analysis of
175 variance (ANOVA) and Tukey's HSD post hoc test. Correlations between different strains and
176 physiochemical indicators were evaluated by the Pearson correlation coefficient. The DIAMOND
177 software tool (<https://github.com/bbuchfink/diamond>) was used to compare our non-redundant gene
178 set with the NR database, with species annotation derived from the corresponding taxonomic database.
179 The Kruskal-Wallis H rank sum test was used to determine significant species across treatments.

180 **3. Results and discussion**

181 **3.1. Distinct structures and responses of intestinal and epidermal bacteria**

182 According to the annotation of the microbiome, 45 and 242 phyla were identified in the intestine
183 and on the epidermis, respectively, indicating that the species richness on the epidermis was higher
184 than that in the intestine. Dissimilarities were observed between the intestinal bacteria and epidermal
185 bacteria of earthworms (Fig. 1A). Owing to the intestinal microenvironment, the bacteria primarily
186 (over 80% in total) included Chloroflexi, Proteobacteria, Acidobacteriota, Actinobacteriota,
187 Firmicutes, and Bacteroidota. For the epidermal microorganisms, similar phyla (except
188 Actinobacteriota) were found. The percentages of Proteobacteria, Actinobacteriota, and Bacteroidota
189 on the epidermis were 2.1–5.6 times higher than those in the intestine, while Chloroflexi and
190 Firmicutes were less dominant. A few significant changes were found in intestinal and epidermal
191 microbial communities at the phylum level after exposure to nZVI, TCEP, and their combination. For
192 example, compared with the microbial community of the control group, the relative abundance of
193 Proteobacteria slightly increased from 15.2% to 23.4% after TCEP exposure, whereas Firmicutes
194 respectively decreased from 10.9% to 2.4% and 5.1% after TCEP exposure and nZVI-TCEP
195 coexposure. Firmicutes on the epidermis also decreased from 4.5% to 2.2% after nZVI-TCEP
196 coexposure. These findings indicate a dysbiosis of microbial community in the intestine and
197 epidermis under the contaminated condition, highlighting the vulnerability of specific phylum such
198 as Firmicutes [23,24]. Overall, the intestinal and epidermal microbiomes shared certain dominant
199 species at the phylum level, while the structures of the two bacterial communities and their responses
200 to soil contamination were distinct.

201

202 **Fig. 1. The intestinal and epidermal bacterial communities at the phylum level after exposure**
203 **to nZVI, TCEP, and nZVI-TCEP. (A) Histogram analyses of species compositions in the**
204 **earthworm gut/on the earthworm epidermis; (B) Cluster analyses of earthworm intestinal**
205 **bacterial communities; (C) Cluster analyses of earthworm epidermal bacterial communities.**

206 Cluster analyses were used to compare the response patterns of bacteria communities after
207 exposure to nZVI, TCEP, and their combination (nZVI-TCEP). As shown in Fig. 1B, the response
208 pattern of intestinal bacteria communities in the control group was closest to that in the nZVI-TCEP
209 coexposure group, indicating that the impact of nZVI-TCEP coexposure on the intestinal bacteria
210 communities was lower than that in the individual exposure groups. The nZVI exposure group located
211 between the nZVI-TCEP coexposure group and the TCEP exposure group, and the TCEP exposure

212 group was far from the control group, implying that the disrupting effect of TCEP on intestinal
213 bacteria communities was stronger than that of nZVI. For epidermal bacteria (Fig. 1C), the combined
214 exposure group exhibited the most significant impact, which was consistent with our previous finding
215 that nZVI and TCEP induced synergistic toxicity in earthworms [19]. This result implied that the
216 response mode of epidermal bacteria was more accordant with host toxicity than that of intestinal
217 microorganisms. Previous studies also proved that the disturbances of environmental pollutants to
218 earthworm epidermal microbiota were complex and variable, depending on the specific abilities of
219 microorganisms. For instance, the relative abundance of *Sorangium* and *Fluviicola* significantly
220 declined after exposure to 5,000 mg/kg nZVI, which is well known for its cellulose-dissolving
221 properties [25] and nitrate nitrogen utilization [26]. To establish the relationship between the
222 microbial response and host toxicity, we further investigated the correlation between the abundance
223 of key species of intestinal/epidermal bacteria and the host physiochemical endpoints.

224 3.2. Epidermal microorganisms exhibited high correlations with joint toxicity in earthworms

225 At the genus level, 29 bacterial genera in the intestine showed significant changes after exposure
226 to nZVI, TCEP, or nZVI-TCEP co-exposure. Among the top 15 genera, 5 and 3 were classified under
227 Proteobacteria and Firmicutes, respectively (Fig. 2A). Existing research suggests that *Tumebacillus*
228 can augment the degradation of sulfamethoxazole (SMX) [27] and *Halocella* is an anaerobic and
229 halophilic bacterium with cellulose decomposition capabilities [28]. *Luteimonas* is known for its
230 robust resistance to pollutants and the metabolic capability of various substrates [29]. The increase in
231 these microbes implied the adaptation of earthworm intestinal bacteria to nZVI and TCEP. Meanwhile,
232 among the epidermal microbes, 357 genera exhibited significant alterations at the genus level. Fig.
233 2B shows that among the top 15 known genera, *Microbacterium*, *Agromyces*, *Mesorhizobium*, *Ensifer*,
234 and *Kaistia* had relatively higher abundances. Importantly, the mean proportions of these genera all
235 exhibited certain increases after exposure to nZVI, TCEP, and nZVI-TCEP, indicating that these
236 epidermal microorganisms positively responded to the contaminations.

237

238 **Fig. 2. Major bacterial communities and their relationship with the host toxicological endpoints**
239 **after exposure to nZVI, TCEP, and nZVI-TCEP. (A) Histogram of multispecies difference test**
240 **at the genus level of earthworm intestinal bacterial communities; (B) Histogram of multispecies**
241 **difference test at the genus level of earthworm epidermal bacterial communities, *P* values**
242 **present significant differences between genera in multiple samples; (C) Pearson correlation**

243 analyses between physiological and biochemical indices and different genera of intestinal
244 bacteria of earthworms at the genus level; (D) Pearson correlation analyses between
245 physiological and biochemical indices and different genera of intestinal bacteria of earthworms
246 at the genus level; the data of physiochemical indices in earthworms is provided in Fig. S2; the
247 yellow area points to the available points of correlation analysis physiological and biochemical
248 indices and bacterial genera.

249 According to the Pearson correlation analysis between the physiochemical indices of
250 earthworms and the top 15 intestinal microorganisms (Fig. 2C), there were nine pairs of highly
251 positive correlations and nine pairs of highly negative correlations, which occupied merely 15% of
252 the total points. The two principal microorganisms were *Tumebacillus* and *f_Bacillaceae*.
253 Concurrently, between epidermal bacteria and the physiochemical indices of earthworms (Fig. 2D),
254 there were 23 pairs of highly positive correlations and 31 pairs of highly negative correlations,
255 accounting for as much as 45% of the total points. The eight key microorganisms included
256 *Microbacterium*, *Mesorhizobium*, *f_Verrucomicrobiaceae*, *Ensifer*, *Kaistia*, *c_Verrucomicrobiae*,
257 *Brevundimonas*, and *o_Verrucomicrobiales*. These results, for the first time, demonstrated the
258 correlations between symbiotic bacteria and host toxicity under a typical soil contamination scenario
259 and indicate that the response of the epidermal bacterial community was much closer to host toxicity
260 than that of the intestinal bacterial community.

261 3.3. Epidermal microorganisms aggravated toxicity in earthworms by robbing metal elements 262 and nutrients

263 The inner link between epidermal microbial community and host toxicity lies in the specific
264 abilities of microorganisms. Among the eight key bacterial genera identified in the present study,
265 *Brevundimonas*, *Microbacterium*, *Mesorhizobium*, and *Ensifer* are well-known heterotrophic
266 microorganisms whose specific functions are associated with elemental utilization, nutrient uptake,
267 and pollutant transformation (Fig. 3 A). In detail, according to the literature investigation (references
268 and details are provided in Table S1), *Brevundimonas* sp., known for their metal tolerance, have been
269 reported as plant growth-promoting rhizobacterial strains with functions such as elemental utilization
270 and sludge remediation [30, 31]. *Microbacterium* sp. are specifically good at the utilization of metal
271 elements (Ca, Fe, Cu, Zn, Ni, Mn, etc.) as well as the hydrolysis of carbohydrates, amino acids and
272 even organic pollutants such as organophosphorus (OP) pesticides, polycyclic aromatic hydrocarbon

273 (PAH), and aflatoxin B1 (AFB1) [32-34]. *Mesorhizobium* sp. consistently demonstrate functions
274 mostly relevant to heavy metal resistance and usage [35, 36]. *Ensifer* sp. are similar to *Brevundimonas*
275 sp., whose functions are also involved in utilizing a wide range of elements and carbohydrates as
276 sources for growth [37, 38]. *Kaistia* sp. are famous for its resistance and degradation abilities to
277 organic pollutants such as phenol and 4-chlorophenol [39, 40]. In this study, it was noted that TCEP
278 concentrations in earthworms showed no significant increases under the coexposure of nZVI and
279 TCEP (Fig. S7), therefore excluding the possibility of synergistic toxicity via pollutant transformation
280 or bioaccumulation. Thus, we further investigated the possibility of element and nutrient uptake as
281 toxicological mechanisms of epidermal microorganism-related host toxicity at the genetic and gene
282 expression levels.

283 Major and trace elements are crucial for the survival and metabolism of both heterotrophic
284 microorganisms and their hosts [41]. Element uptake by epidermal microorganisms from the host
285 could be conducted through several mechanisms, such as ion exchange, chelation, and reduction
286 processes [42,43], mainly controlled by metal-responsive proteins [44-46]. As shown in Fig. 3B and
287 Table S3, the abundance of the *Fur* gene could be induced by both nZVI and TCEP exposure, which
288 significantly increased by 4.72-fold ($P < 0.01$) under the coexposure condition. Similarly, the *ScaC*
289 gene was upregulated by nZVI (1.49-fold, $P < 0.05$) and TCEP (2.80-fold, $P < 0.01$), as well as nZVI-
290 TCEP coexposure (4.14-fold, $P < 0.01$). The protein products of the *Fur* gene and *ScaC* gene are
291 involved in the uptake of Fe^{2+} [47], indicating that the epidermal microbial community tended to
292 enhance Fe element storage abilities after coexposure to nZVI and TCEP. Although the *MntR* gene
293 exhibited no significant changes, the *Fur* gene-encoded protein can also bind Mn^{2+} to form Mn-Fur
294 complex [48,49]. Such overlapped Mn uptake function might also result in the decrease of Mn content
295 in the host earthworms. Different from *Fur* paralogs, *CueR* gene encodes a copper efflux regulon and
296 is involved in the negative regulation of Cu storage [50]. In our study, the *CueR* gene was significantly
297 decreased after exposure to nZVI (0.68-fold, $P < 0.01$) and nZVI-TCEP (0.56-fold, $P < 0.01$),
298 indicating that the Cu storage was also enhanced [51,52]. Overall, these findings suggested epidermal
299 microbial communities tended to strengthen their metal elements uptake and storage when facing
300 nZVI, TCEP, and especially their coexposure.

301 Previous evidence showed that symbiotic microorganisms could loot metal elements from hosts
302 and affect the homeostasis of host elements, thus influencing the pollution tolerance of the host via
303 specific functional proteins. For example, many pathogenic/nonpathogenic Gram-negative and

304 Gram-positive bacteria can acquire iron by using host iron compounds such as heme and transferrin,
305 which may further regulate host health [12]. To further confirm the coupling relationship between
306 microbial element uptake functions and host toxicity, six major elements (Na, K, Ca, P, Mg, and Fe)
307 (Fig. S1) and three trace elements (Zn, Mn, and Cu) (Fig. 4A-C) in the host earthworms were
308 investigated. It was found that Ca, P, and Mg contents in earthworms remained steady, while Na and
309 K displayed a slight increase (Fig. S8), potentially linked to muscle tissue atrophy and an elevated
310 osmotic pressure of intracellular fluid [53]. Notably, the metal elements, including Zn, Cu, Mn, and
311 Fe, in the host earthworms all showed declines after nZVI and TCEP coexposure (Fig. 4B and S3,
312 Table S4). In detail, Zn contents slightly decreased from 0.26 to 0.23 mg/g body weight (bw) after
313 exposure to 5,000 µg/kg TCEP, while under the coexposure condition, the value was as low as 0.18
314 mg/g bw ($P < 0.01$). Such Zn deficiency may cause immune organ shrinkage and lymphocyte
315 reduction in animals [54,55]. The Mn contents in earthworms were sensitive to TCEP exposure, with
316 values decreasing from 0.37 to 0.26, 0.20, and 0.18 mg/g bw after exposure to 50, 500, and 5,000
317 µg/kg TCEP and 0.25, 0.21, and 0.19 mg/g bw after exposure to 50, 500, and 5,000 µg/kg TCEP and
318 5,000 mg/kg nZVI, respectively. The Cu content also decreased from 0.30 to approximately 0.20
319 mg/g bw after exposure to 5,000 µg/kg TCEP and high-dose nZVI-TCEP coexposure, and the Fe
320 content significantly decreased from 467 to 271 and 74 mg/g bw after coexposure to 500 and 5,000
321 µg/kg TCEP and 5,000 mg/kg nZVI. These decreases of Zn, Mn, Cu, and Fe contents in the host
322 earthworms were highly consistent with the significantly altered abundance of *Fur*, *ScaC*, and *CueR*
323 in the epidermal microbial communities along with their multiple metal ion uptake functions [48, 49].
324 Moreover, Zn, Cu, Mn, and Fe are known as cofactors for various cellular functions, such as energy
325 metabolism and antioxidant enzymes [51,56,57]. For example, Zn-, Mn- and Cu-superoxide
326 dismutase (SOD) catalyzes the dismutation of the superoxide anion and is a metalloenzyme
327 ubiquitous to living organisms [57], and the decreased metal element contents were consistent with
328 the suppressed antioxidative abilities in the host reported in our previous study [19]. These findings
329 indicate that heterotrophic epidermal microorganisms tended to upregulate their uptake abilities of
330 metal elements from the host, which may be responsible for the weakened stress tolerance of
331 earthworms.

332

333 **Fig. 3. Reported functions of key species and the relative abundance of related genes after**
334 **exposure to nZVI, TCEP, and nZVI-TCEP. (A) A chord map of reported category of microbial**

335 **functions summarized from literature (Table S1); (B) Gene expressions related to metal-**
336 **responsive proteins (*Fur*, *CueR*, *ScaC*, and *MntR*) and saccharides/amino acids uptake (*Bgl*,**
337 ***LacZ*, *NocR*, and *PabcT*). *Fur*, Ferric uptake regulator; *CueR*, Cu(I)-responsive transcriptional**
338 **regulator; *ScaC*, scaffoldin anchoring protein C; *MntR*, Mn²⁺ transporter; *Bgl*, beta-glucosidase;**
339 ***LacZ*, beta-galactosidase; *NocR*, nucleoid occlusion protein regulatory protein; *PabcT*, Peptide**
340 **ABC transporter.**

341 It is also noted that *Brevundimonas*, *Microbacterium*, and *Ensifer* have specific capabilities
342 related to the uptake of saccharides and amino acids [58-60]. These substances, usually provided by
343 the host, are essential nutrients and energy sources for the survival of heterotrophic bacteria [44-46].
344 As shown in Fig. 3B, the *Bgl* and *LacZ* genes involved in the uptake and utilization of D-glucose and
345 lactose were upregulated by 2.84–3.73-fold ($P < 0.01$) after individual exposure to nZVI and TCEP.
346 Moreover, *Bgl*, *LacZ*, and *PabcT* all positively responded to the coexposure of nZVI and TCEP,
347 peaking at 4.11–7.86-fold ($P < 0.01$). Meanwhile, the corresponding contents of D-glucose, lactose,
348 and glutamine in earthworms showed significant decreases ($P < 0.01$) in a synergistic manner after
349 exposure to nZVI, TCEP, and their combination (Fig. 4D-F and Table S4). In detail, D-glucose
350 contents were sensitive to nZVI but not TCEP, which decreased from 314 to 272, 234, and 211 $\mu\text{mol/g}$
351 protein after exposure to 50, 500, and 5,000 mg/kg nZVI ($P < 0.05$), respectively. Under the
352 coexposure condition, these values were as low as 183, 203, and 162 $\mu\text{mol/g}$ protein ($P < 0.01$).
353 Lactose contents in earthworms were also sensitive to nZVI exposure, with the value significantly
354 decreasing from 9.97 to 4.90 and 2.08 mg/g bw after exposure to 500 and 5,000 mg/kg nZVI ($P <$
355 0.01) and 1.61, 1.42, and 1.40 mg/g bw after exposure to 50, 500, and 5,000 $\mu\text{g/kg}$ TCEP and 5,000
356 mg/kg nZVI ($P < 0.01$). In contrast, glutamine contents were sensitive to TCEP exposure, decreasing
357 from 37 to 32 and 28 $\mu\text{mol/g}$ protein after exposure to 500 and 5,000 $\mu\text{g/kg}$ TCEP and 24–19 $\mu\text{mol/g}$
358 protein under nZVI-TCEP coexposure, respectively. The decreases in nutrients as energy sources
359 were coincident with the upregulated uptake abilities in the key microorganisms, which may be
360 related to the deterioration of host vulnerability [61-64] and thus induce synergistic toxicities under
361 nZVI and TCEP co-contamination. Taken together, it might be possible that key epidermal
362 microorganisms may avail themselves of the opportunity to obtain metal elements and nutrients from
363 earthworms when facing multiple contaminants and thus contribute to the malnutrition of the host at
364 the physiochemical level.

365

366 **Fig. 4. Contents of metal elements and nutrients in earthworms after exposure to nZVI, TCEP,**
367 **and nZVI-TCEP. (A) Zn, (B) Mn, (C) Cu, (D) D-glucose, (E) lactose, and (F) glutamine. * and #**
368 **represent the significance among different nZVI and TCEP treatments (*, # $P < 0.05$, **, ## $P < 0.01$).**

369 4. Conclusions

370 This study compared the distinct responses of intestinal and epidermal microorganism
371 communities in earthworms under a typical co-contamination scenario. It was found that intestinal
372 and epidermal microorganisms were mostly composed of heterotrophic anaerobic bacteria sharing
373 similar phyla, but the species and functions were different at the genus level. Notably, the community
374 changes of epidermal microbes exhibited higher correlations with host toxicity than that of intestinal
375 microbes. Facing the co-exposure of nZVI and TCEP, a shift in the microbial community occurred,
376 with heterotrophic epidermal microorganisms that possess special functions of metal elements and
377 nutrient utilization becoming dominant. This shift was accompanied by a substantial increase in the
378 abundance of metal and nutrient uptake genes such as *Fur*, *ScaC*, *Bgl*, and *LacZ*. These changes might
379 be responsible for the deficiency of corresponding substances in host earthworms. The combined
380 pollution scenario simulated in this study is a representative scenario, and the intricate interactions
381 between the epidermal microorganisms and the host are worthy of further investigation.

382 Author contributions

383 **J.H.:** conceptualization, data curation, experiment, writing–original draft, funding acquisition.

384 **M.R.Y.:** experiment, data curation, formal analysis, writing–original draft. **X.Y.W. and Y.Q.L.:**

385 writing–review & editing. **Q.Q.C.:** data curation, formal analysis. **J.Y.Z.:** resources. **D.H.L.:**

386 writing–review & editing, supervision, funding acquisition.

387 Declaration of Competing Interests

388 The authors declare that there are no conflicts of interest in the present experiment.

389 Acknowledgements

390 This work was supported by the National Key Research and Development Program of China
391 (2022YFC3702103), the Natural Science Foundation of China (U21A20163, 42192573, 22376181)
392 and the Zhejiang Provincial Natural Science Foundation of China (LD21B070001).

393 References

394 [1] G. Caballero-Flores, J.M. Pickard, G. Núñez, Microbiota-mediated colonization resistance:

- 395 mechanisms and regulation, *Nat. Rev. Microbiol.* 21 (2023) 347-360,
396 <https://doi.org/10.1038/s41579-022-00833-7>.
- 397 [2] Z. Chen, J. Dolfing, S. Zhuang, Y. Wu, Periphytic biofilms-mediated microbial interactions and
398 their impact on the nitrogen cycle in rice paddies, *Eco-Environ. Health* 1 (2022) 172-180,
399 <https://doi.org/10.1016/j.eehl.2022.09.004>.
- 400 [3] E.G. Ruby, Symbiotic conversations are revealed under genetic interrogation, *Nat. Rev.*
401 *Microbiol.* 6 (2008) 752-762, <https://doi.org/10.1038/nrmicro1958>.
- 402 [4] R.M. Medina-Sauza, M. Álvarez-Jiménez, A. Delhal, F. Reverchon, M. Blouin, J.A. Guerrero-
403 Analco, C.R. Cerdán, R. Guevara, L. Villain, I. Barois, Earthworms building up soil microbiota,
404 a review, *Front. Environ. Sci.* 7 (2019) 81, <https://doi.org/10.3389/fenvs.2019.00081>.
- 405 [5] P. Gebrayel, C. Nicco, S. Al Khodor, J. Bilinski, E. Caselli, E.M. Comelli, M. Egert, C. Giaroni,
406 T.M. Karpinski, I. Loniewski, et al., Microbiota medicine: towards clinical revolution, *J. Transl.*
407 *Med.* 20 (2022) 111, <https://doi.org/10.1186/s12967-022-03296-9>.
- 408 [6] N. Wang, W. Wang, Y. Jiang, W. Dai, P. Li, D. Yao, J. Wang, Y. Shi, Z. Cui, H. Cao, et al.,
409 Variations in bacterial taxonomic profiles and potential functions in response to the gut transit
410 of earthworms (*Eisenia fetida*) feeding on cow manure, *Sci. Total. Environ.* 787 (2021) 147392,
411 <https://doi.org/10.1016/j.scitotenv.2021.147392>.
- 412 [7] B. De Pessemier, L. Grine, M. Debaere, A. Maes, B. Paetzold, C. Callewaert, Gut-Skin Axis:
413 Current knowledge of the interrelationship between microbial dysbiosis and skin conditions,
414 *Microorganisms* 9 (2021) 353, <https://doi.org/10.3390/microorganisms9020353>.
- 415 [8] Z. Iliodromiti, A.R. Triantafyllou, M. Tsaousi, A. Pouliakis, C. Petropoulou, R. Sokou, P. Volaki,
416 T. Boutsikou, N. Iacovidou, Gut microbiome and neurodevelopmental disorders: A link yet to
417 be disclosed, *Microorganisms* 11 (2023) 487, <https://doi.org/10.3390/microorganisms11020487>.
- 418 [9] H. Y. Deng, Y. L. Tu, H. Wang, Z. Y. Wang, Y. Y. Li, L. Y. Chai, W. C. Zhang, Z. Lin,
419 Environmental behavior, human health effect and pollution control of heavy metal (loid)s toward
420 full life cycle processes, *Eco-Environ. Health* 1 (2022) 229-243,
421 <https://doi.org/10.1016/j.eehl.2022.11.003>.
- 422 [10] X. Liu, Y. Wang, H. Xiang, J. Wu, X. Yan*, W. Zhang*, Z. Lin, L. Chai, Unveiling the crucial
423 role of iron mineral phase transformation in antimony(V) elimination from natural water, *Eco-*
424 *Environ. Health* 2 (2023) 176-183, <https://doi.org/10.1016/j.eehl.2023.07.006>.
- 425 [11] C. Zhang, X. He, Y. Sheng, C. Yang, J. Xu, S. Zheng, J. Liu, W. Xu, Y. Luo, K. Huang, Allicin-

- 426 induced host-gut microbe interactions improves energy homeostasis, *FASEB J.* 34 (2020)
427 10682-10698, <https://doi.org/10.1096/fj.202001007R>.
- 428 [12] Y. Seyoum, K. Baye, C. Humblot, Iron homeostasis in host and gut bacteria - a complex
429 interrelationship, *Gut Microbes* 13 (2021) e187485,
430 <https://doi.org/10.1080/19490976.2021.1874855>.
- 431 [13] J. Zhang, L. Zhang, M. He, Y. Wang, C. Zhang, D. Lin, Bioresponses of earthworm-microbiota
432 symbionts to polychlorinated biphenyls in the presence of nano zero valent iron in soil, *Sci. Total.*
433 *Environ.* 856 (2023) 159226, <https://doi.org/10.1016/j.scitotenv.2022.159226>.
- 434 [14] Y.Y. Yu, D. F. Tong, Y. H. Yu, D. D. Tian, W. Zhou, W. Zhang, X. Zhang, W. Shi, G. Liu, Toxic
435 effects of four emerging pollutants on cardiac performance and associated physiological
436 parameters of the thick-shell mussel (*Mytilus coruscus*), *Environ. Pollut.* 21 (2023) 122244,
437 <https://doi.org/10.1016/j.envpol.2023.122244>.
- 438 [15] J. Hou, C. Hu, J. C. White, K. Yang, L. Z. Zhu, D. H. Lin, Nano-zoo interfacial interaction as a
439 design principle for hybrid soil remediation technology, *ACS Nano* 15 (2021) 14954-14964,
440 <https://doi.org/10.1021/acsnano.1c05180>.
- 441 [16] X. Ge, S. Ma, X. Zhang, Y. Yang, G. Li, Y. Yu, Halogenated and organophosphorous flame
442 retardants in surface soils from an e-waste dismantling park and its surrounding area:
443 Distributions, sources, and human health risks. *Environ. Inter.* 139 (2020) 105741,
444 <https://doi.org/10.1016/j.envint.2020.105741>.
- 445 [17] T. Tosco, M. P. Papini, C. C. Viggi, R. Sethi, Nanoscale zerovalent iron particles for groundwater
446 remediation: A review. *J. Clean. Prod.* 77 (2014) 10-21,
447 <https://doi.org/10.1016/j.jclepro.2013.12.026>.
- 448 [18] W. Wan, S. Zhang, H. Huang, T. Wu, Occurrence and distribution of organophosphorus esters in
449 soils and wheat plants in a plastic waste treatment area in China. *Environ. Pollut.* 214 (2016)
450 349-353, <https://doi.org/10.1016/j.envpol.2016.04.038>.
- 451 [19] M. Yang, X. Wu, C. He, J. Zhang, J. Hou, D. Lin, nZVI-induced iron poisoning aggravated the
452 toxicity of TCEP to earthworm in soil, *Environ. Pollut.* 317 (2023) 120785,
453 <https://doi.org/10.1016/j.envpol.2022.120785>.
- 454 [20] K.J. Livak, T.D. Schmittgen, Analysis of relative gene expression data using real-time
455 quantitative PCR and the $2^{-\Delta\Delta Ct}$ method, *Methods* 25 (2001) 402-408,
456 <https://doi.org/10.1006/meth.2001.1262>.

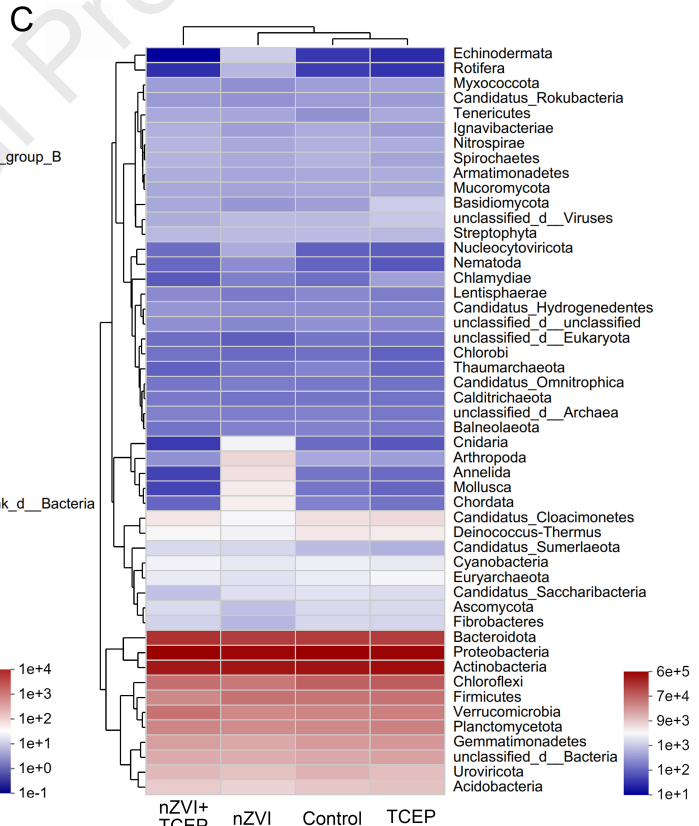
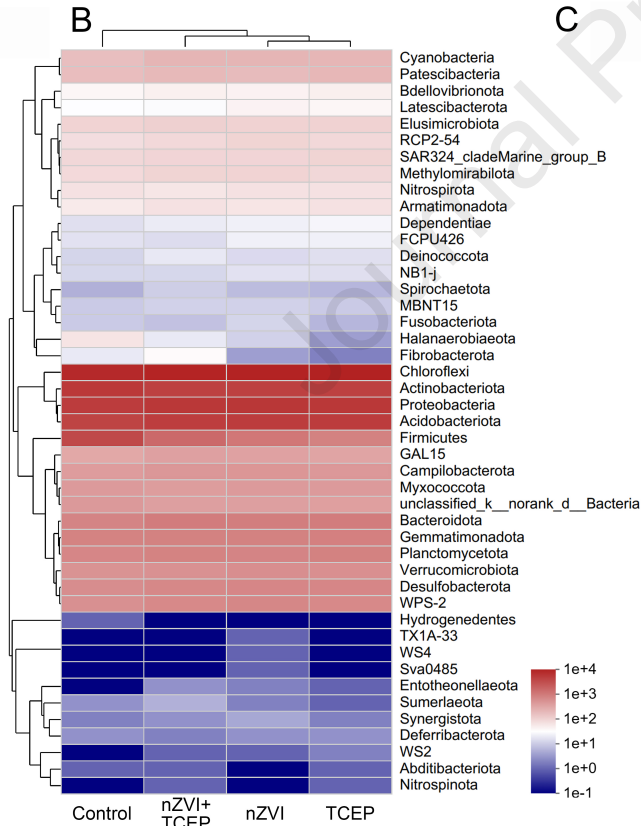
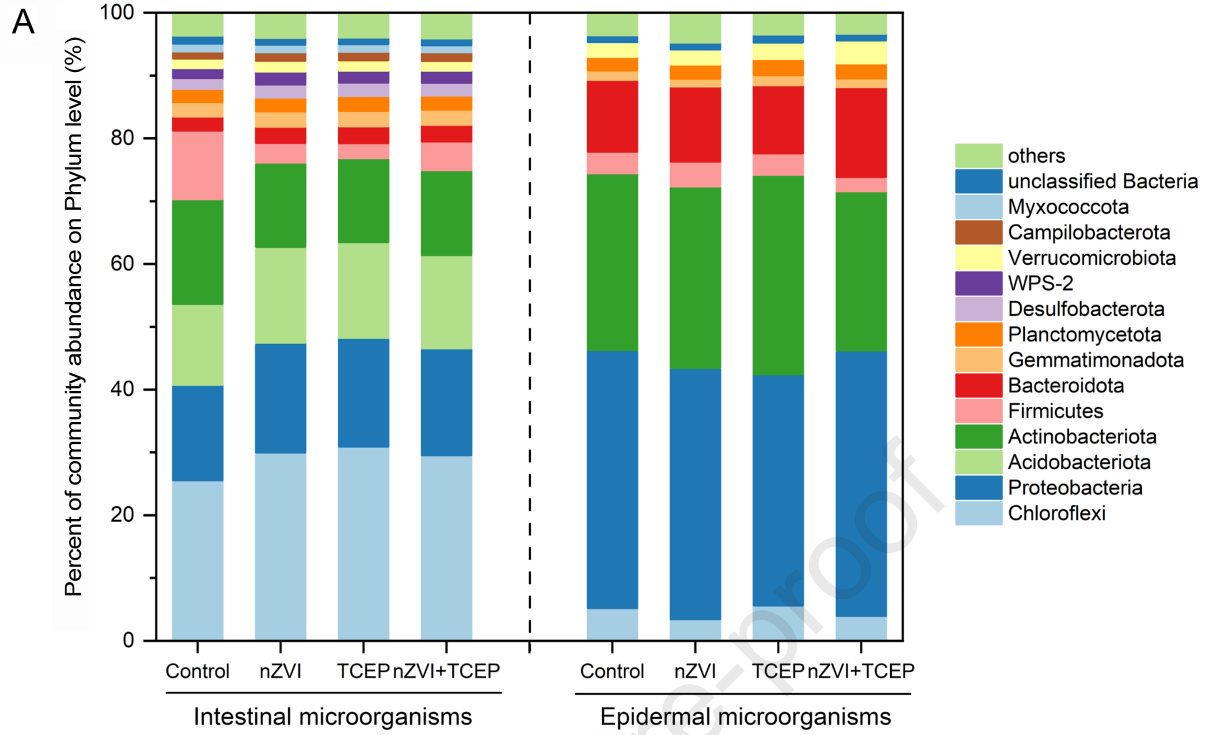
- 457 [21] R. Visvanathan, C. Jayathilake, R. Liyanage, R. Sivakanesan, Applicability and reliability of the
458 glucose oxidase method in assessing α -amylase activity. Food Chem. 275 (2019) 265-272,
459 <https://doi.org/10.1016/j.foodchem.2018.09.114>.
- 460 [22] Q. Zhou, W. Lin, C. Wang, F. Sun, S. Ju, Q. Chen, Y. Wang, Y. Chen, H. Li, L. Wang, et al.,
461 Neddylation inhibition induces glutamine uptake and metabolism by targeting CRL3^{SPOP} E3
462 ligase in cancer cells, Nat. Commun. 13 (2022) 3034, [https://doi.org/10.1038/s41467-022-](https://doi.org/10.1038/s41467-022-30559-2)
463 [30559-2](https://doi.org/10.1038/s41467-022-30559-2).
- 464 [23] N.R. Shin, T.W. Whon, J.W. Bae, Proteobacteria: microbial signature of dysbiosis in gut
465 microbiota, Trends Biotechnol. 33 (2015) 496-503,
466 <https://doi.org/10.1016/j.tibtech.2015.06.011>.
- 467 [24] S. Filippidou, T. Wunderlin, T. Junier, N. Jeanneret, C. Dorador, V. Molina, D.R. Johnson, P.
468 Junier, A combination of extreme environmental conditions favor the prevalence of endospore-
469 forming firmicutes, Front Microbiol. 7 (2016) 1707, <https://doi.org/10.3389/fmicb.2016.01707>.
- 470 [25] K.I. Mohr, C. Wolf, U. Nubel, A.K. Szafranska, M. Steglich, F. Hennesen, K. Gemperlein, P.
471 Kampfer, K. Martin, R. Muller, et al., A polyphasic approach leads to seven new species of the
472 cellulose-decomposing genus Sorangium, *Sorangium ambruticinum* sp. nov.; *Sorangium arenae*
473 sp. nov.; *Sorangium bulgaricum* sp. nov.; *Sorangium dawidii* sp. nov.; *Sorangium kenyense* sp.
474 nov.; *Sorangium orientale* sp. nov. and *Sorangium reichenbachii* sp. nov., Int. J. Syst. Evol.
475 Microbiol. 68 (2018) 3576-3586, <https://doi.org/10.1099/ijsem.0.003034>.
- 476 [26] Y.B. Zhang, Y.L. Wang, W.H. Li, L.N. Bao, L.H. Wang, X.H. Huang, B. Huang, Biogas emission
477 from an anaerobic reactor, Aerosol. Air Qual. Res. 18 (2018) 1493-1502,
478 <https://doi.org/10.4209/aaqr.2018.05.0169>.
- 479 [27] Y. Zhang, K. Song, J. Zhang, X. Xu, G. Ye, H. Cao, M. Chen, S. Cai, X. Cao, X. Zheng, et al.,
480 Removal of sulfamethoxazole and antibiotic resistance genes in paddy soil by earthworms
481 (*Pheretima guillelmi*): Intestinal detoxification and stimulation of indigenous soil bacteria, Sci.
482 Total. Environ. 851 (2022) 158075, <https://doi.org/10.1016/j.scitotenv.2022.158075>.
- 483 [28] Z. Xie, X. Meng, H. Ding, Q. Cao, Y. Chen, X. Liu, D. Li, The synergistic effect of rumen
484 cellulolytic bacteria and activated carbon on thermophilic digestion of cornstalk, Bioresour.
485 Technol. 338 (2021) 125566, <https://doi.org/10.1016/j.biortech.2021.125566>.
- 486 [29] Y. Mu, Y. Pan, W. Shi, L. Liu, Z. Jiang, X. Luo, X.C. Zeng, W.J. Li, *Luteimonas arsenica* sp.
487 nov.: An arsenic-tolerant bacterium isolated from arsenic-contaminated soil, Int. J. Syst. Evol.

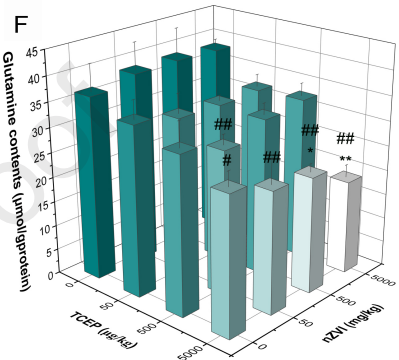
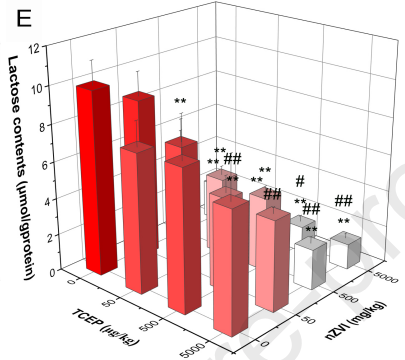
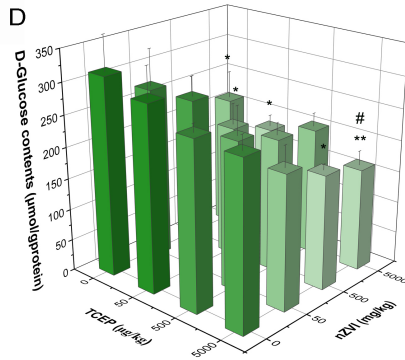
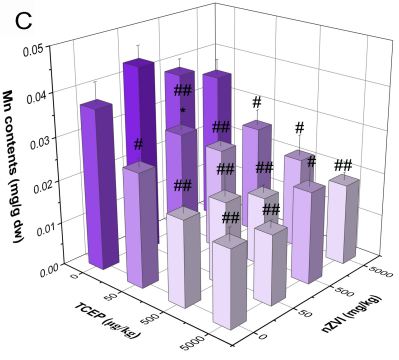
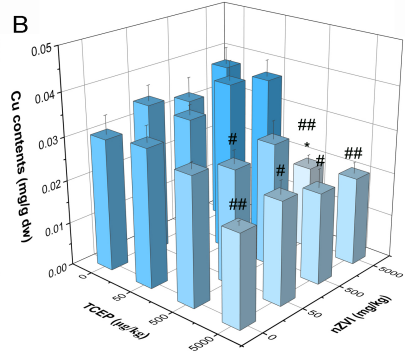
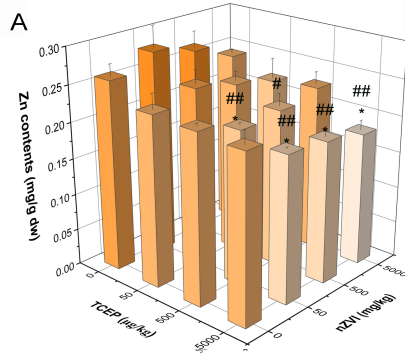
- 488 Microbiol. 66 (2016) 2291-2296, <https://doi.org/10.1099/ijsem.0.001024>.
- 489 [30] P. Sharma, P. Chaturvedi, R. Chandra, S. Kumar, Identification of heavy metals tolerant
490 *Brevundimonas sp.* from rhizospheric zone of *Saccharum munja* L. and their efficacy in in-situ
491 phytoremediation, *Chemosphere* 295 (2022) 133823,
492 <https://doi.org/10.1016/j.chemosphere.2022.133823>.
- 493 [31] N. Singh, N. Marwa, S.K. Mishra, J. Mishra, P.C. Verma, S. Rathaur, N. Singh, *Brevundimonas*
494 *diminuta* mediated alleviation of arsenic toxicity and plant growth promotion in *Oryza sativa* L,
495 *Ecotoxicol. Environ. Saf.* 125 (2016) 25-34, <https://doi.org/10.1016/j.ecoenv.2015.11.020>.
- 496 [32] H. Karlidag, A. Esitken, M. Turan, F. Sahin, Effects of root inoculation of plant growth
497 promoting rhizobacteria (PGPR) on yield, growth and nutrient element contents of leaves of
498 apple, *Sci. Hortic.* 114 (2007) 16-20, <https://doi.org/10.1016/j.scienta.2007.04.013>.
- 499 [33] L. Panneerselvan, K. Krishnan, S.R. Subashchandrabose, R. Naidu, M. Megharaj, Draft genome
500 sequence of *Microbacterium esteraromaticum* MM1, a bacterium that hydrolyzes the
501 organophosphorus pesticide fenamiphos, isolated from golf course soil, *Microbiol. Resour.*
502 *Announc.* 7 (2018) e00862-18, <https://doi.org/10.1128/MRA.00862-18>.
- 503 [34] Y. Yan, X. Zhang, H. Chen, W. Huang, H. Jiang, C. Wang, Z. Xiao, Y. Zhang, J. Xu, Isolation
504 and aflatoxin B1-degradation characteristics of a *Microbacterium proteolyticum* B204 strain
505 from bovine faeces, *Toxins* 14 (2022) 525, <https://doi.org/10.3390/toxins14080525>.
- 506 [35] M. Fan, Z. Liu, L. Nan, E. Wang, W. Chen, Y. Lin, G. Wei, Isolation, characterization, and
507 selection of heavy metal-resistant and plant growth-promoting endophytic bacteria from root
508 nodules of *Robinia pseudoacacia* in a Pb/Zn mining area, *Microbiol. Res.* 217 (2018) 51-59,
509 <https://doi.org/10.1016/j.micres.2018.09.002>.
- 510 [36] T. Bohu, C.M. Santelli, D.M. Akob, T.R. Neu, V. Ciobota, P. Rosch, J. Popp, S. Nietzsche, K.
511 Kusel, Characterization of pH dependent Mn(II) oxidation strategies and formation of a bixbyite-
512 like phase by *Mesorhizobium australicum* T-G1, *Front. Microbiol.* 6 (2015) 734,
513 <https://doi.org/10.3389/fmicb.2015.00734>.
- 514 [37] Y. Wang, W. Chen, L. He, Q. Wang, X.F. Sheng, Draft genome sequence of *Ensifer adhaerens*
515 M78, a mineral-weathering bacterium isolated from soil, *Genome Announc.* 4 (2016) e00969-
516 16, <https://doi.org/10.1128/genomeA.00969-16>.
- 517 [38] G. Rocha, A. Le Quere, A. Medina, A. Cuellar, J.L. Contreras, R. Carreno, R. Bustillos, J.
518 Munoz-Rojas, M.D.C. Villegas, C. Chaintreuil, et al., Diversity and phenotypic analyses of salt-

- 519 and heat-tolerant wild bean *Phaseolus filiformis* rhizobia native of a sand beach in Baja
520 California and description of *Ensifer aridi* sp. nov., Arch. Microbiol. 202 (2020) 309-322,
521 <https://doi.org/10.1007/s00203-019-01744-7>.
- 522 [39] L. Jin, K.K. Kim, H.G. Lee, C.Y. Ahn, H.M. Oh, *Kaistia defluvii* sp. nov. isolated from river
523 sediment, Int. J. Syst. Evol. Microbiol. 62 (2012) 2878-2882,
524 <https://doi.org/10.1099/ijs.0.038687-0>.
- 525 [40] H.W. Lee, H.S. Yu, Q.M. Liu, H.M. Jung, S.T. Lee, *Kaistia granuli* sp. nov. isolated from
526 anaerobic granules in an upflow anaerobic sludge blanket reactor, Int. J. Syst. Evol. Microbiol.
527 57 (2007) 2280-2283, <https://doi.org/10.1099/ijs.0.65023-0>.
- 528 [41] B.M. Mitrović, S. Stefanović, D. Šefer, D. Jovanović, J. Ajtić, The content of ten elements in pig
529 feed and manure and its relationship with element concentration in earthworms on swine farms,
530 Toxin Rev. 42 (2023) 332-341, <https://doi.org/10.1080/15569543.2022.2163662>.
- 531 [42] T. Bohu, C.M. Santelli, D.M. Akob, T.R. Neu, V. Ciobota, P. Rosch, J. Popp, S. Nietzsche, K.
532 Kusel, Characterization of pH dependent Mn(II) oxidation strategies and formation of a bixbyite-
533 like phase by *Mesorhizobium australicum* T-G1, Front. Microbiol. 6 (2015) 734,
534 <https://doi.org/10.3389/fmicb.2015.00734>.
- 535 [43] S. Verma, M. Kumar, A. Kumar, S. Das, H. Chakdar, A. Varma, A.K. Saxena, Diversity of
536 bacterial endophytes of maize (*Zea mays*) and their functional potential for micronutrient
537 biofortification, Curr. Microbiol. 79 (2021) 6, <https://doi.org/10.1007/s00284-021-02702-7>.
- 538 [44] S. H. Choi, K.L. Lee, J. H. Shin, Y. B. Cho, S. S. Cha, J. H. Roe, Zinc-dependent regulation of
539 zinc import and export genes by *zur*, Nat. Comm. 8 (2017) 15812,
540 <https://doi.org/10.1038/ncomms15812>.
- 541 [45] J. Lan, Y. Sun, X. Chen, W. Zhan, Y. Du, T.C. Zhang, H. Ye, D. Du, H. Hou, Bio-leaching of
542 manganese from electrolytic manganese slag by *Microbacterium trichothecenolyticum* Y1:
543 Mechanism and characteristics of microbial metabolites, Bioresour. Technol. 319 (2021) 124056,
544 <https://doi.org/10.1016/j.biortech.2020.124056>.
- 545 [46] H. Naz, R.Z. Sayyed, R.U. Khan, A. Naz, O.A. Wani, A. Maqsood, S. Maqsood, A. Fahad, S.
546 Ashraf, P.L. Show, *Mesorhizobium* improves chickpea growth under chromium stress and
547 alleviates chromium contamination of soil, J. Environ. Manage. 338 (2023) 117779,
548 <https://doi.org/10.1016/j.jenvman.2023.117779>.
- 549 [47] J. W. Lee, J. D. Helmann, Functional specialization within the Fur family of metalloregulators.

- 550 Biometals 20 (2007) 485-499, <https://doi.org/10.1007/s10534-006-9070-7>.
- 551 [48] E. Sevilla, M. T. Bes, M. L. Peleato, M. F. Fillat, Fur-like proteins: Beyond the ferric uptake
552 regulator (Fur) paralog. Arch. Biochem. Biophys. 701 (2021) 108770,
553 <https://doi.org/10.1016/j.abb.2021.108770>.
- 554 [49] M. Y. Hamed, J. B. Neilands. An electron spin resonance study of the Mn(II) and Cu(II)
555 complexes of the Fur repressor protein. J. Inorg. Biochem. 53 (1994) 235-248,
556 [https://doi.org/10.1016/0162-0134\(94\)85111-5](https://doi.org/10.1016/0162-0134(94)85111-5).
- 557 [50] F. W. Outten, C. E. Outten, J. Hale, T. V. O'Halloran, Transcriptional activation of an *Escherichia*
558 *coli* copper efflux regulon by the chromosomal MerR homologue, CueR. J. Bio. Chem. 275 (2000)
559 31024-31029, <https://doi.org/10.1074/jbc.M006508200>.
- 560 [51] K.J. Waldron, N.J. Robinson, How do bacterial cells ensure that metalloproteins get the correct
561 metal?, Nat. Rev. Microbiol. 7 (2009) 25-35, <https://doi.org/10.1038/nrmicro2057>.
- 562 [52] T. Kajikawa, R. Sugiyama, K. Kataoka, T. Sakurai, A novel resting form of the trinuclear copper
563 center in the double mutant of a multicopper oxidase, CueO, Cys500Ser/Glu506Ala, J. Inorg.
564 Biochem. 149 (2015) 88-90, <https://doi.org/10.1016/j.jinorgbio.2015.03.005>.
- 565 [53] B.F. Palmer, Regulation of potassium homeostasis, Clin. J. Am. Soc. Nephrol. 10 (2015) 1050-
566 1060, <https://doi.org/10.2215/CJN.08580813>.
- 567 [54] W. Maret, Zinc biochemistry: from a single zinc enzyme to a key element of life, Adv. Nutr. 4
568 (2013) 82-91, <https://doi.org/10.3945/an.112.003038>.
- 569 [55] Y. Higashimura, T. Takagi, Y. Naito, K. Uchiyama, K. Mizushima, M. Tanaka, M. Hamaguchi,
570 Y. Itoh, Zinc deficiency activates the il-23/th17 axis to aggravate experimental colitis in mice, J.
571 Crohns Colitis 14 (2020) 856-866, <https://doi.org/10.1093/ecco-jcc/jjz193>.
- 572 [56] X. Zhao, W. Liu, Z. Cai, B. Han, T. Qian, D. Zhao, An overview of preparation and applications
573 of stabilized zero-valent iron nanoparticles for soil and groundwater remediation, Water Res.
574 100 (2016) 245-266, <https://doi.org/10.1016/j.watres.2016.05.019>.
- 575 [57] E.A.B. Pajarillo, E. Lee, D.K. Kang, Trace metals and animal health: Interplay of the gut
576 microbiota with iron, manganese, zinc, and copper, Anim. Nutr. 7 (2021) 750-761,
577 <https://doi.org/10.1016/j.aninu.2021.03.005>.
- 578 [58] G. Rocha, A. Le Quere, A. Medina, A. Cuellar, J.L. Contreras, R. Carreno, R. Bustillos, J.
579 Munoz-Rojas, M.D.C. Villegas, C. Chaintreuil, et al., Diversity and phenotypic analyses of salt-
580 and heat-tolerant wild bean *Phaseolus filiformis* rhizobia native of a sand beach in Baja

- 581 California and description of *Ensifer aridi* sp. nov, Arch. Microbiol. 202 (2020) 309-322,
582 <https://doi.org/10.1007/s00203-019-01744-7>.
- 583 [59] N. Singh, N. Marwa, S.K. Mishra, J. Mishra, P.C. Verma, S. Rathaur, N. Singh, *Brevundimonas*
584 *diminuta* mediated alleviation of arsenic toxicity and plant growth promotion in *Oryza sativa* L,
585 *Ecotoxicol. Environ. Saf.* 125 (2016) 25-34, <https://doi.org/10.1016/j.ecoenv.2015.11.020>.
- 586 [60] Y. Yan, X. Zhang, H. Chen, W. Huang, H. Jiang, C. Wang, Xiao, Z. Zhang, Y. Xu, J. Isolation
587 and aflatoxin B1-degradation characteristics of a *Microbacterium proteolyticum* B204 strain
588 from bovine faeces, *Toxins* 14 (2022) 525, <https://doi.org/10.3390/toxins14080525>.
- 589 [61] H.M. Ishaq, I.S. Mohammad, R. Hussain, R. Parveen, J. H. Shirazi, Y. Fan, M. Shahzad, K.
590 Hayat, H. Li, A. Ihsan, et al., Gut-Thyroid axis: How gut microbial dysbiosis associated with
591 euthyroid thyroid cancer, *J. Cancer.* 13 (2022) 2014-2028, <https://doi.org/10.7150/jca.66816>.
- 592 [62] J. J. Ni, X. S. Li, H. Zhang, Q. Xu, X. T. Wei, G. J. Feng, M. Zhao, Z. J. Zhang, L. Zhang, G.H.
593 Shen, et al., Mendelian randomization study of causal link from gut microbiota to colorectal
594 cancer, *BMC Cancer* 22 (2022) 1371, <https://doi.org/10.1186/s12885-022-10483-w>.
- 595 [63] Z.J. Zhang, H.L. Qu, N. Zhao, J. Wang, X.Y. Wang, R. Hai, B. Li, Assessment of causal direction
596 between gut microbiota and inflammatory bowel disease: A mendelian randomization analysis,
597 *Front. Genet.* 12 (2021) 631061, <https://doi.org/10.3389/fgene.2021.631061>.
- 598 [64] X. Wang, X. Yang, F. Zhou, Z. Tian, J. Cheng, J. P. Michaud, X. Liu, Symbiotic bacteria on the
599 cuticle protect the oriental fruit moth *Grapholita molesta* from fungal infection, *Biol. Control*
600 169 (2022) 104895, <https://doi.org/10.1016/j.biocontrol.2022.104895>.





Highlights

- Contributions of intestinal and epidermal microorganisms in host toxicity were compared.
- Epidermal microbes exhibited higher correlations with host toxicity than intestinal microbes.
- Certain heterotrophic epidermal microorganisms became superior after co-exposure.
- Consumption of elements and nutrients by the microbes contributed to the malnutrition in host.

Journal Pre-proof